Online Observation of Structure Information of Mixed-Gas Hydrate Containing High Concentration of CO2 Based on Raman Spectroscopy

Baoyong Zhang[1,2], Yue Yu[1,2*], Xia Gao[3], Qiang Wu[1,2], and Chuanhai Liu[1,2]

[1] Department of Safety Engineering, Heilongjiang University of Science and Technology, Harbin 150022, Heilongjiang China
[2] National Professional Center Lab of Safety Basic Research for Hydrocarbon Gas Pipeline Transportation Network, Harbin 150022, Heilongjiang, China
[3] Department of Architectural and Civil Engineering, Heilongjiang University of Science of Technology, Harbin 150022, China
[*] Corresponding author. E-mail: yuyue@iem.ac.cn

Received: Sept. 02, 2021; Accepted: Oct. 18, 2021

The research on the micro crystal structure of coal mine gas (CMG) hydrate is especially significant for the technology of gas hydrate separation. Raman spectroscopy is an effective method for on-line analysis of gas hydrate microstructure. Using Raman spectroscopy to observe the microstructure of mixed-gas hydrate crystals formed by three kinds of gas samples under two driving forces, which contain a high concentration of carbon dioxide. This experiment obtained information about the hydrate crystals, including large and small cage occupancy, and obtained the hydration number indirectly based on the statistical thermodynamic model of van der Waals and Platteeuw. The results show that the large cages of hydrate phases are nearly fully occupied by carbon dioxide and methane molecules together, with the occupancy ratios between 97.70% and 98.70%. Most of the guest molecules in large cages are carbon dioxide (75.82% $\sim$ 94.00%) and only a few are filled with methane (4.70% $\sim$ 31.50%). However, the small cage occupancy ratios are generally low, in the range from 18.28% to 66.06%, and the guest molecules are all methane. The cage occupancy, both large and small, which methane occupied, increased as the methane concentration in the gas sample increased. However, the large cage occupancy, which methane occupied, is lower than the small cage. In addition, the hydration number of three kinds of gas samples in different systems is from 6.38 to 7.32. The occupancy of small cavities increased as the methane concentration in the coal mine gas sample increased, while the hydration number decreased.

Keywords: Gas hydrate; Raman spectrum; Cage occupancy; Hydration numbe

http://dx.doi.org/10.6180/jase.202208_25(4).0006

---

1. Introduction

As a clean energy, coal mine gas (CMG) has been widely used around the world. However, the utilization of CMG is still low in some areas because it contains a high concentration of carbon dioxide, but methane concentration is low. This kind of CMG needs to separate and purify methane from the CMG mixture before being used. The gas hydrate separation technology could not only separate and purify methane from the CMG mixture, but it could also directly control carbon dioxide discharged into the atmosphere, preventing the greenhouse effect from intensifying [1–4].

The fundamental structure of gas hydrate is that water molecules are bonded to each other by hydrogen bonds to form cage holes in which gas molecules are enveloped to form envelope compounds. The gas storage capacity is the key research point of gas hydration separation technology and an important parameter for measuring the gas storage capacity of hydrate [5–7]. Gas storage capacity is determined by the hydration number. The molecular formula of hydrate is $M{\cdot}nH_2O$, "n" is hydration number [8, 9]. As a basic research method, micro laser Raman spectroscopy can accurately obtain the chemical composition, crystal structure, cage occupancy, and hydration number of the sample without interference from surrounding substances [10–13].

Using Raman spectroscopy, X-ray, and NMR, researchers carried out a lot of research on the crystal structure and other information about hydrates compounded in the laboratory and existing in nature. This avoided the complicated calculation process of some parameters [14–17]. The hydration number of pure CH_4 hydrate measured by Uchida et al. [8] is basic at 6.2. Large cages CH_4 occupied is more than small cages. A series of hydration numbers of CH_4 hydrate obtained by Liu et al. [16] and Liu et al. [18] in different systems of synthesis in the laboratory ranges from 6.05 to 6.15, but the sample of natural gas hydrate recovered from the Shenhu Area in the South China Sea is closer to the theoretical value (5.99 ± 0.04). Gborigi et al. [9] determined the presence of CO_2 in both the liquid and hydrate forms of the composite, and the hydration number is low (2.15–3.60); this may be attributed to the high fraction of water-filled pores in the hydrate composite. Sum et al. [19] measured two vapor compositions of the CH_4 + CO_2 system; the large cages are nearly completely occupied by both CH_4 and CO_2 , whereas only a small fraction of the small cages are occupied by CH_4, and the hydration number is 7.27-7.45. This test result is more close to Huai-yan et al. [20]. Subramanian et al. [21] obtained the hydration number of the CH_4+C_2H_6 system (6.51-7.66), and the large cage occupancy is higher too. For complex multivariate mixed systems, Prasad and Kiran [12] demonstrated the existence of mixed hydrates, even under low-pressure. Prasad et al. [22] also suggest that it needs to be combined with other techniques to confirm cage occupancy. To summarize, the hydration number is influenced not only by growing conditions, but also by the test method and calculation method.

Using an online testing experiment platform for CMG hydrate built by the laboratory, we could use Raman spectroscopy to make a nondestructive evaluation of the hydrate. Meanwhile, we could avoid the trouble that gas hydrate is easy to decompose under normal pressure. This paper intends to conduct online testing to obtain the structure information of a mixed-gas hydrate containing a high concentration of CO_2. The final goal is to get more crystal information and the transformation law, and therefore accelerate the gas hydrate technique industrialization.

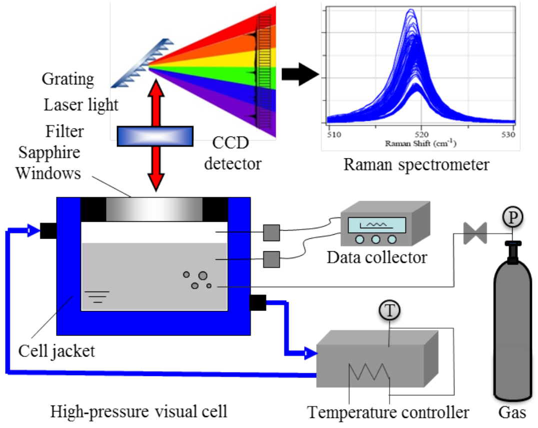

Fig. 1. In-situ test system of gas hydrate reaction

2. Experimental

2.1. Equipment and reagents

Based on the Confocal Visible Microscope Raman Spectrometer of LabRAM HR800 produced by Horiba Jobin Yovin of France, we built the online testing experiment platform for CMG hydrate. It consists of a Raman Spectrometer, an in-situ reaction kettle, a constant temperature system, a gas sample charging system, and a data acquisition system.

The in-situ reaction kettle made of stainless steel is equipped with sapphire windows to ensure the laser passes through completely and easily observes the reaction process, with 3 ml of effective volume, and the maximum test pressure attains up to 20 MPa, as shown in Fig. 1. Six experiments were conducted in this paper. The main reagents were the distilled water (lab homemade) and the CMG containing a high concentration of CO_2 (supplied by Harbin Liming Gas Co., Ltd.). The gas composition was chosen so that it represents the industrial composition. The experimental system is shown in Table 1.

2.2. Gas hydrate preparation

Inject distilled water into the reaction kettle and then use the constant temperature system to adjust the temperature of the reaction kettle. When the temperature of the reaction kettle drops to 2 °C, charge the gas sample into the kettle until it reaches the required pressure, then stew the kettle and observe the pressure change. After waiting for the kettle's inside pressure to remain constant, let it stand for 3 days and then begin the spectrum test.

2.3. Spectrometer parameters

The lateral resolution of the Raman Spectrometer is lower than 2 μm; and it's equipped with a 785 nm and a 532

Table 1. The initial conditions of gas hydrate reaction experiment

Gas sample	volume of the solution/ml	initial temperature/°C	initial pressure/MPa
G1	1.5	2	4.8 (ΔP=3.0) 5.3 (ΔP=3.5)
G2			4.9 (ΔP=3.0) 5.4 (ΔP=3.5)
G3			5.0 (ΔP=3.0) 5.5 (ΔP=3.5)

Note: G1: 80%CO2+6%CH4+14%N2;
G2: 75%CO2+11%CH4+14%N2;
G3: 70%CO2+16%CH4+14%N2.

nm laser. Scattering light is collected in backscatter geometry and dispersed off of 1800 and 600 gv/mm gratings. A 50x telephoto lens and software from Labspec are also equipped.

2.4. Test condition and method

The Raman shift of the molecule is related to the vibration and rotation level only and has nothing to do with the frequency of incident light, and the intensity of the spectral is proportional to the intensity of incident light and sample concentration. This is why the Raman Spectrometer could provide qualitative and quantitative analysis of the molecular structure of gas hydrate as a basic research method. 50x telephoto lens, 532 nm laser, 400 μm confocal hole, 200 μm slit, and 60s integral time are the experimental conditions. Before the test, a monocrystalline silicon piece (Raman peak at 520.7 cm^{-1}) was used to check the Raman spectrometer first in order to get more accurate Raman spectral information. The Raman spectroscopy test focuses on the peak of CO2 and CH4 hydrate phase, so the collection interval of the Raman peak is from 500 cm^{-1} to 1900 cm^{-1} and from 2300 cm^{-1} to 3900 cm^{-1}.

3. Results and Analysis

The change process of the gas and liquid phases in the reaction kettle was observed during the experimental process. Typical images of gas sample 2 (5.4 MPa) during the experiment process were shown in Figure 2. When experiments were carried out for 5 min, white hydrate particles appeared on the gas-liquid interface in the kettle, as shown in Fig. 2(a), and the experimental pressure at this time was 5.26 MPa. With the process of reaction, white glacial hydrate occur area increased, and the liquid phase dropped off, shown in Fig. 2(b). With further response, system pressure approached equilibrium, and there was no liquid phase to be seen inside the kettle. The hydration reaction was complete, as shown in Fig. 2(c).

3.1. Raman spectra of gas phase

Continuous testing work was carried out on gas samples of two kinds of driving force in six experimental systems during the hydration process. The test result is shown in Fig. 3. Because CO_2 is a linear molecule, it has four kinds of modes of vibration: symmetrical stretching vibration $v1$, antisymmetric stretching vibration $v3$, and tow bending vibrations $v2$ and $v4$ [23]. Because Fermi resonance exists in CO_2 molecules, this causes a hybrid excited state division and the Fermi resonance bimodal form. The Fermi resonance bimodal presents two characteristic spectral bands in the Raman spectra, and the high frequency is at 1386 cm^{-1}, and the low frequency is at 1282 cm^{-1} [23, 24]. The thermal spikes produced by the transition state lie on both sides of two spectral lines. The spectrum of symmetrical stretching vibration $v1$ of the C-H bond in the CH_4 gas molecule measured in the experiment presented a signal at 2916 cm^{-1}; the spectrum of stretching vibration of the N-N bond in the N_2 gas molecule presented a signal at 2324 cm^{-1}. The peak area histogram of the gas molecule is shown in Fig. 4. The Raman spectra of the carbon dioxide spectrum peak intensity is the largest, followed by the methane spectral peak, and the lowest is the nitrogen spectral peak, and the concentration range of three kinds of gas in the gas sample, from large to small, are carbon dioxide, methane, nitrogen, so it can be seen that the peak area and the gas concentration were positively related in the figure.

3.2. Raman spectra of hydrate phase

The basic structural characteristics of cage hydrate are that the host molecules (water) are connected in space through hydrogen bonds to form polyhedral pores of different sizes, and the pores develop into cage hydrate lattices through vertex or plane connections. There are usually three types of crystal structure in gas hydrate: structure I, structure II and structure H. Normally, small guest molecules whose molecular diameter is 4.2 $\sim$ 6 Å such as CH_4, CO_2, et al., can only occupy the hydrate cavity of structure I and form metastable hydrates of structure I. The Raman spectra of

Fig. 2. The typical photos of hydrate formation process

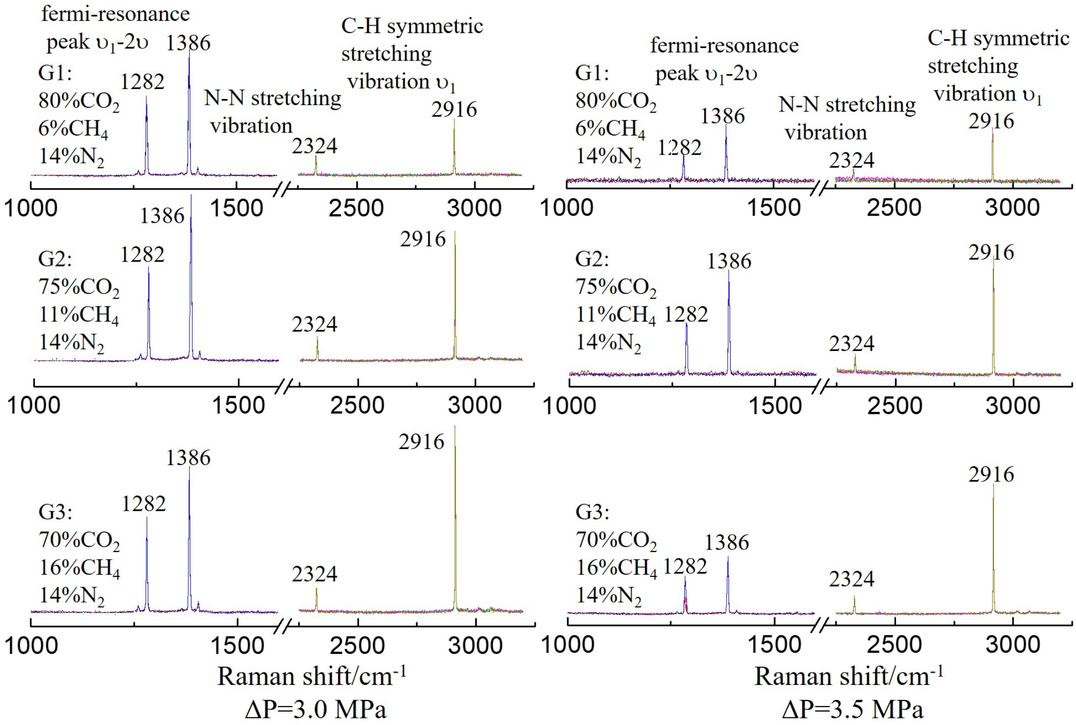

Fig. 3. Raman spectra of gas phase

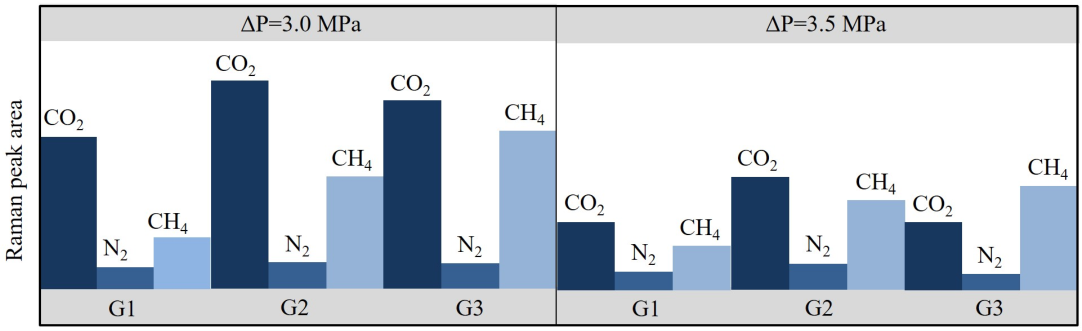

Fig. 4. Peak area histogram of gas molecule

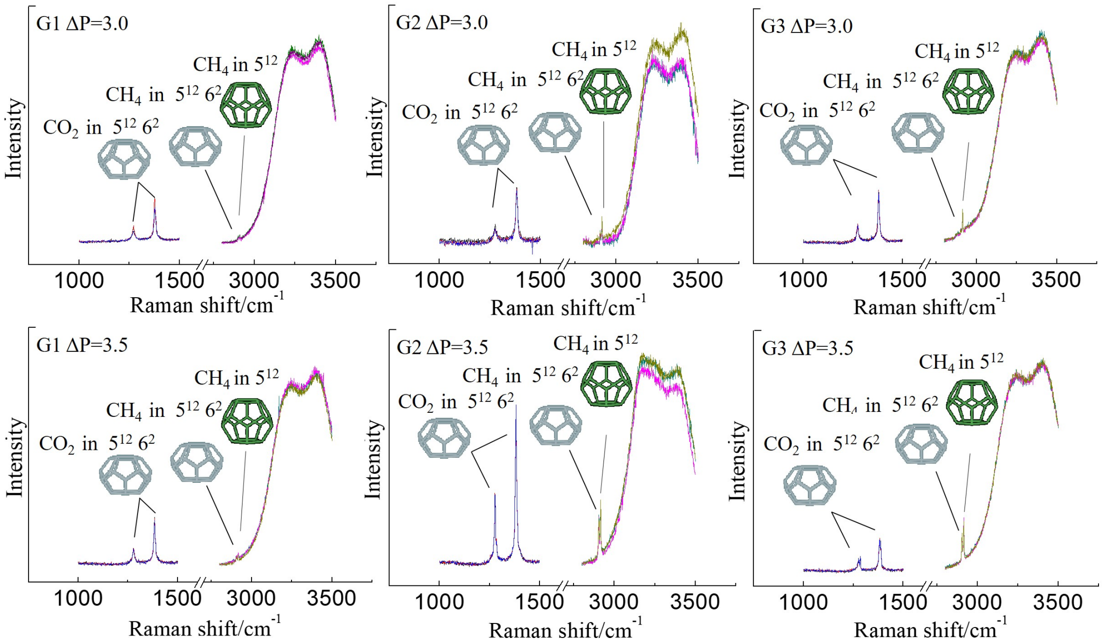

Fig. 5. Raman spectra of CO_2-CH_4 gas hydrate

the 6 group hydrate phase in two kinds of thermodynamic conditions is shown in Fig. 5. The Raman spectra reveal the presence of two Raman shifts at low wave numbers (1279 cm^{-1} and 1383 cm^{-1}). The two Raman shifts are the Fermi resonance bimodal of CO_2 molecules in the hydrate phase [24], and it's the CO_2 molecules which occupied the large cavity of structure I [19, 25]. The CH_4 molecule has two Raman shifts too, 2904 cm^{-1} and 2915 cm^{-1}. According to the loose cage-tight cage model [26], compared with gas molecules of CH_4, the C-H band adjustable frequency of CH_4 molecules caught in "loose cage" (large cavity) has a "blue shift", but the C-H band adjustable frequency of CH_4 molecules caught in "tight cage" (small cavity) is close to the gas phase. So 2901 cm^{-1} is the CH_4 molecule occupied in the large cavity, and 2915 cm^{-1} is the CH_4 molecule occupied in the small cavity.

The result of the hydration reaction experiment showed that consumption of CO_2 gas formed hydrate of structure I and occupied the large cavity only. Preliminary analysis shows the molecular dimension of CO_2 gas is too large to occupy the small cavity of the structure I in this thermodynamic condition. CH_4 molecules could occupy both large and small cavities of structure I.

3.3. Hydration number (n)

The molecular formula of gas hydrate in structure I is $8M{\cdot}46H_2O$, which can also be written as $M{\cdot}5.75H_2O$. Therefore, the theoretical value of hydration number is 5.75, concluding 46 water molecules, composed of 6 large cavities and 2 small cavities. Based on the statistical thermodynamic model of van der Waals and Platteeuw, we can confirm cage occupancy and hydration number in the CO_2-CH_4 system.

$$\theta_L/\theta_S = I_L/3I_S \mapsto$$

$$\Delta\mu_{w,H} = -\frac{RT}{23}\left[3\ln\left(1-\theta_{L,CO_2}-\theta_{L,CH_4}\right)+\right.$$

$$\left.\ln\left(1-\theta_{s,CO_2}-\theta_{s,CH_4}\right)\right]$$

$$n = 23/\left(3\theta_{L,CO_2}+3\theta_{L,CH_4}+\theta_{s,CO_2}+\theta_{S,CH_4}\right)$$

Where θ_L and θ_S are the fractional occupancy of large and small cavities respectively, I_L and I_S are the Raman spectra intensity of large and small cavities respectively, $\Delta\mu_{W,H}$ is the chemical potential difference of water in hydrate lattice and liquid water, used in the calculation was 1297 J/mol.

In order to obtain the changes in cage occupancy and hydration number during the growth of the CMG hydrate phase, Raman spectral curves of each growth stage are integrated to obtain the corresponding peak area data. According to the peak areas corresponding to the Raman displacement of the three CMG samples at different moments of hydrate growth, the relative occupancy rates of each cage in the hydrate of the CO_2-CH_4 binary system can be determined ($\theta_{S,CH_4}/\theta_{S,CO_2}$, $\theta_{L,CH_4}/\theta_{L,CO_2}$, $\theta_{L,CH_4}/\theta_{S,CH_4}$ and $\theta_{L,CO_2}/\theta_{S,CO_2}$). Then, the cage occupancy and hydration number of CMG hydrate in each system were obtained.

The experimental results are shown in Table 2. The result shows that under the two kinds of driving force,

Table 2. Hydration numbers and cage occupancies of gas hydrate in different system

*Delta*P/MPa	Gas sample	$\theta_{L,CO_2}/\%$	$\theta_{L,CH_4}/\%$	$\theta_{S,CH_4}/\%$	hydration number (n)
3.0	G1	94.00	4.70	18.28	7.32
	G2	67.02	31.50	33.87	6.98
	G3	75.82	22.75	29.93	7.14
3.5	G1	93.37	5.23	22.12	7.23
	G	90.06	8.46	32.42	7.01
	G3	81.08	17.07	66.06	6.38

the large cavity of gas hydrate is nearly filled with guest molecules, and the cage occupancy changed little (97.70%$\sim$ 98.70%); among them, CO_2 is the vast majority (75.82% $\sim$ 94.00%), and only a little CH_4 (4.70% $\sim$ 31.50%). The small cage occupancy is generally low (18.28% $\sim$ 66.06%), and all of them are CH_4. The preliminary analysis shows that the low concentration of CH_4 in the CMG sample leads to a low occupancy rate of CH_4 molecules in large and small cavities. In the calculation results, with the increase of CH4 concentration in the gas sample, the occupancy of CH_4 molecules in both large and small cavities increased, and the occupancy of CH_4 molecules in large cavities is lower than that in small cavities. This may be because CO_2 and CH_4 molecules occupy large cavities together in the CO_2-CH_4 system of this thermodynamic condition, so there is a competitive relationship between the two kinds of gas molecules and CO_2 concentration is higher than CH_4 concentration. Some of the CH_4 molecules could occupy small cavities smoothly. So this kind of result appeared. In addition, the hydration number of three kinds of gas samples in different systems is from 6.38 to 7.32. The occupancy of small cavities increased as the CH_4 concentration in the CMG sample increased, while the hydration number decreased. And with the increase in driving force, the hydration number of hydrates formed by the three gas samples showed a decreasing trend. This suggests that the higher driving force helps to enhance the gas storage capacity of gas hydrate.

4. Conclusion

Raman spectroscopy is an effective method for on-line analysis of gas hydrate microstructure. The crystal microstructure of CMG hydrate at different times of growth was observed by the Raman spectroscopy online test platform. The cage occupancy was measured and the hydration number and other structural information were obtained indirectly.

In the experiments, large cavities were nearly fully filled; occupancy of large cavities was maintained from 97.70% to 98.70% and changed little. Most of the gas molecules occupying large cavities are CO_2 (75.82% $\sim$ 94.00%). CH_4 molecules are only a little (4.70% $\sim$ 31.50%). Occupancy of small cavities is generally low (18.28%$\sim$ 66.06%) and only occupied by CH_4 molecules. With the increase in CH_4 concentration in the gas sample, the occupancy of CH_4 molecules in both large and small cavities increased, and the occupancy of CH_4 molecules in large cavities is lower than that in small cavities. In addition, the hydration number of three kinds of gas samples in different systems is from 6.38 to 7.32. The occupancy of small cavities increased as the CH_4 concentration in the CMG sample increased, while the hydration number decreased. And with the increase in driving force, the hydration number of these three kinds of gas samples decreased.

Online Raman spectroscopy observation technology can accurately determine the molecular structure and other information of gas hydrate and reveal the transformation law of gas hydrate microstructure. This has certain guiding significance for research on the formation and decomposition mechanisms of gas hydrates and for realizing industrial applications of the technology of gas hydrate separation.

This study only discussed the Raman spectrum information of the mixed-gas hydrate formed by three kinds of gas samples under two driving forces, which contained a high concentration of CO_2 in the preliminary. We still need further study to obtain more detailed crystal structure information, transformation law, and influence mechanism of gas hydrate.

Acknowledgments

The work reported in this paper was funded by the National Natural Science Foundation of China under NSFC Contract No. 51774123, 51704103 and 51974112. Heilongjiang Province Natural Science Foundation of China (E2016058). Special thanks are due to the National Professional Center Lab of Safety Basic Research for Hydrocarbon Gas Pipeline Transportation Network, Heilongjiang University of Science & Technology in China.

References

[1] B. Samset, J. Fuglestvedt, and M. Lund, (2020) *"Delayed emergence of a global temperature response after* *emission mitigation"* **Nature Communications** ***11***(1): DOI: 10.1038/s41467-020-17001-1.

[2] C. Zheng, B. Jiang, S. Xue, Z. Chen, and H. Li, (2019) *"Coalbed methane emissions and drainage methods in underground mining for mining safety and environmental benefits: A review"* **Process Safety and Environmental Protection** ***127***: 103–124. DOI: 10.1016/j.psep.2019.05.010.

[3] W. Wang, H. Li, Y. Liu, M. Liu, H. Wang, and W. Li, (2020) *"Addressing the gas emission problem of the world's largest coal producer and consumer: Lessons from the Sihe Coalfield, China"* **Energy Reports** ***6***: 3264–3277. DOI: 10.1016/j.egyr.2020.11.199.

[4] N. Gaikwad, J. Sangwai, P. Linga, and R. Kumar, (2021) *"Separation of coal mine methane gas mixture via sII and sH hydrate formation"* **Fuel** ***305***: DOI: 10.1016/j.fuel.2021.121467.

[5] S. Daghash, P. Servio, and A. Rey, (2020) *"Elastic properties and anisotropic behavior of structure-H (sH) gas hydrate from first principles"* **Chemical Engineering Science** ***227***: DOI: 10.1016/j.ces.2020.115948.

[6] X.-Y. Zeng, J.-R. Zhong, Y.-F. Sun, S.-L. Li, G.-J. Chen, and C.-Y. Sun, (2017) *"Investigating the partial structure of the hydrate film formed at the gas/water interface by Raman spectra"* **Chemical Engineering Science** ***160***: 183–190. DOI: 10.1016/j.ces.2016.11.012.

[7] P. Chattaraj, S. Bandaru, and S. Mondal, (2011) *"Hydrogen storage in clathrate hydrates"* **Journal of Physical Chemistry A** ***115***(2): 187–193. DOI: 10.1021/jp109515a.

[8] T. Uchida, T. Hirano, T. Ebinuma, H. Narita, K. Gohara, S. Mae, and R. Matsumoto, (1999) *"Raman spectroscopic determination of hydration number of methane hydrates"* **AIChE Journal** ***45***(12): 2641–2645. DOI: 10.1002/aic.690451220.

[9] M. Gborigi, D. Riestenberg, M. Lance, S. McCallum, Y. Atallah, and C. Tsouris, (2007) *"Raman spectroscopy of a hydrated CO2/water composite"* **Journal of Petroleum Science and Engineering** ***56***(1-3): 65–74. DOI: 10.1016/j.petrol.2005.09.005.

[10] H. Truong-Lam, S. Cho, and J. Lee, (2019) *"Simultaneous in-situ macro and microscopic observation of CH4 hydrate formation/decomposition and solubility behavior using Raman spectroscopy"* **Applied Energy** ***255***: DOI: 10.1016/j.apenergy.2019.113834.

[11] Y. Hiraga, T. Sasagawa, S. Yamamoto, H. Komatsu, M. Ota, T. Tsukada, and J. Smith R.L., (2020) *"A precise deconvolution method to derive methane hydrate cage occupancy ratios using Raman spectroscopy"* **Chemical Engineering Science** ***214***: DOI: 10.1016/j.ces.2019.115361.

[12] P. Prasad and B. Kiran, (2020) *"Stability and exchange of guest molecules in gas hydrates under the influence of CH4, CO2, N2 and CO2+N2 gases at low-pressures"* **Journal of Natural Gas Science and Engineering** ***78***: DOI: 10.1016/j.jngse.2020.103311.

[13] Q. Lv and X. Li. "Raman Spectroscopic Studies on Microscopic Mechanism of CP - CH4 Mixture Hydrate". In: ***142***. 2017, 3264–3269. DOI: 10.1016/j.egypro.2017.12.501.

[14] T. Makino, Y. Ogura, Y. Matsui, T. Sugahara, and K. Ohgaki, (2009) *"Isothermal phase equilibria and structural phase transition in the carbon dioxide + cyclopropane mixed-gas hydrate system"* **Fluid Phase Equilibria** ***284***(1): 19–25. DOI: 10.1016/j.fluid.2009.05.020.

[15] H. Joon Shin, Y.-J. Lee, J.-H. Im, K. Won Han, J.-W. Lee, Y. Lee, J. Dong Lee, W.-Y. Jang, and J.-H. Yoon, (2009) *"Thermodynamic stability, spectroscopic identification and cage occupation of binary CO2 clathrate hydrates"* **Chemical Engineering Science** ***64***(24): 5125–5130. DOI: 10.1016/j.ces.2009.08.019.

[16] C. Liu, Y. Ye, Q. Meng, Z. Lu, Y. Zhu, J. Liu, and S. Yang, (2010) *"Raman spectroscopic characteristics of natural gas hydrate recovered from Shenhu Area in South China Sea and Qilian mountain permafrost"* **Acta Chimica Sinica** ***68***(18): 1881–1886.

[17] S.-P. Kang and J.-W. Lee, (2013) *"Hydrate-phase equilibria and 13C NMR Studies of Binary (CH4+ C2H4) and (C2H6+ C2H4) hydrates"* **Industrial & Engineering Chemistry Research** ***52***(1): 303–308.

[18] C.-L. Liu, Y.-G. Ye, and Q.-G. Meng, (2010) *"Determination of hydration number of methane hydrates using micro-laser Raman spectroscopy"* **Guang Pu Xue Yu Guang Pu Fen Xi/Spectroscopy and Spectral Analysis** ***30***(4): 963–966. DOI: 10.3964/j.issn.1000-0593(2010)04-0963-04.

[19] A. Sum, R. Burruss, and E. Sloan Jr., (1997) *"Measurement of clathrate hydrates via Raman spectroscopy"* **Journal of Physical Chemistry B** ***101***(38): 7371–7377. DOI: 10.1021/jp970768e.

[20] L. Huai-yan, G. Bao-cong, L. Jian-hui, and L. Zhen, (2005) *"Coupled relationship among hydrate structure, hydration number, and Raman spectrum"* **Geoscience** ***19***(1): 83.

[21] S. Subramanian, R. Kini, S. Dec, and E. Sloan Jr., (2000) *"Evidence of structure II hydrate formation from methane + ethane mixtures"* **Chemical Engineering Science *55***(11): 1981–1999. DOI: 10.1016/S0009-2509(99)00389-9.

[22] P. Prasad, Y. Sowjanya, and K. Shiva Prasad, (2009) *"Micro-Raman investigations of mixed gas hydrates"* **Vibrational Spectroscopy *50***(2): 319–323. DOI: 10.1016/j.vibspec.2009.02.003.

[23] Y. Garrabos, V. Chandrasekharan, M. Echargui, and F. Marsault-Herail, (1989) *"Density effect on the raman fermi resonance in the fluid phases of CO2"* **Chemical Physics Letters *160***(3): 250–256. DOI: 10.1016/0009-2614(89)87591-8.

[24] Y. Garrabos, M. Echargui, and F. Marsault-Herail, (1989) *"Comparison between the density effects on the levels of the Raman spectra of the Fermi resonance doublet of the 12C16O2 and 13C16O2 molecules"* **The Journal of Chemical Physics *91***(10): 5869–5881. DOI: 10.1063/1.457455.

[25] C. Ratcliffe and J. Ripmeester, (1986) *"Proton and carbon-13 NMR studies on carbon dioxide hydrate"* **The Journal of Physical Chemistry *90***(7): 1259–1263.

[26] S. Subramanian and E. Sloan Jr., (2002) *"Trends in vibrational frequencies of guests trapped in clathrate hydrate cages"* **Journal of Physical Chemistry B *106***(17): 4348–4355. DOI: 10.1021/jp013644h.